Switchable diode effect in ferroelectric thin film: High dependence on poling process and temperature

Z. X. Li,[1,2,3] X. L. Liu,[1,a] W. J. Chen,[2,3] X. Y. Zhang,[2,3] Ying Wang,[2,3] W. M. Xiong,[2,3] and Yue Zheng[2,3,a]

[1]*Shenzhen Key Laboratory of Advanced Materials, Shenzhen Engineering Lab of Flexible Transparent Conductive Films, Department of Materials Science and Engineering, Shenzhen Graduate School, Harbin Institute of Technology, Shenzhen 518055, The People's Republic of China*

[2]*State Key Laboratory of Optoelectronic Materials and Technologies, School of Physics and Engineering, Sun Yat-sen University, 510275, Guangzhou, China*

[3]*Micro&Nano Physics and Mechanics Research Laboratory, School of Physics and Engineering, Sun Yat-sen University, 510275, Guangzhou, China*

(Received 2 September 2014; accepted 24 November 2014; published online 5 December 2014)

$Pb(Zr_{0.53}Ti_{0.47})O_3$ (PZT) thin film was fabricated on $Pt/Ti/SiO_2/Si$ substrate by chemical solution deposition method. Our results show a very great switchable ferroelectric diode effect (SFDE) in Pt-PZT-Au structure, which is more obvious and controllable than that in other ferroelectric thin films. The electrical conduction exhibits high rectifying behavior after pre-poling and the polarity of ferroelectric diode can be switched by changing the orientation of polarization in ferroelectric thin film. Our results also indicate that the SFDE in PZT film is highly dependent on remanent polarization and temperature. With the increase of remanent polarization, the forward current of bistable rectifying behavior observably reduces. Therefore, our measurement indicated that the biggest rectification ratio can reach about 220, which is found in 250K after +10V poling. By analyzing the conduction data, it is found that the dominant conduction mechanism of the SFDE in this sample is due to the space-charge-limited bulk conduction (SCLC), and Schottky emission (SE) may play subordinate role in forward bias voltage. Our observation demonstrates that SFDE may be general characteristic in ferroelectrics as long as proper electrodes chosen. © *2014 Author(s). All article content, except where otherwise noted, is licensed under a Creative Commons Attribution 3.0 Unported License.* [http://dx.doi.org/10.1063/1.4903772]

I. INTRODUCTION

Due to the behavior of the bistable remanent polarization, ferroelectrics have a wide range of applications, especially ferroelectric random access memory (FeRAM). It is high storage density, non-volatile and extremely fast in read/write process.[1] In spite of these advantages, one of the problems in FeRAM is that the read process is destructive. In FeRAM, reading is accomplished by applying a bias to the ferroelectric capacitor and then detecting the polarization-switching current. This process destroys the former information in memory cell, and rewrite process is necessary. In order to realize the full potential of FeRAMs, there are a number of approaches in order to attain FeRAMs with high operation speed and non-destructive readout (NDRO), etc. These include FeRAMs based on ferroelectric photovoltaic effect or interface barrier modulation by defects.[2–5]

Recently, T. Choi *et al.*[6] have studied the photoelectric characteristics in a single crystal $BiFeO_3$ (BFO) with symmetrical Au electrodes, and reported this special thin film with great switchable

[a]Authors to whom correspondence should be addressed. Electronic addresses: zhengy35@mail.sysu.edu.cn and xiangliliu@hit.edu.cn.

 ©Author(s) 2014

All article content, except where otherwise noted, is licensed under a Creative Commons Attribution 3.0 Unported license. See: http://creativecommons.org/licenses/by/3.0/ Downloaded to IP: 113.96.155.10 On: Tue, 09 Dec 2014 06:41:23

ferroelectric diode effect (SFDE). The pre-poled ferroelectric crystal shows a diode like rectifying characteristic when bias voltage is applied within the coercive field. Moreover, it is worth noting that the direction of the diode can be changed by polarization reverse. This novel finding could be very useful for the potential application in a nondestructive readout FeRAM with a simple Metal-Ferroelectric -Metal (MFM) structure. Subsequently, some further researches were accomplished and confirmed that the SFDE also exists in structures with asymmetric electrodes.[7–10] Moreover, a theoretical model predicts that SFDE can be enhanced by proper choice of electrodes, indicating that the chemical component of ferroelectric material is not essential to the appearance of SFDE.[11] Therefore, SFDE should be a general property of MFM systems having electrodes with suitable work function and permittivity. However, this interesting phenomenon has not been reported and comprehensively investigated in other ferroelectric materials except for BFO.

Actually, L. Pintilie *et al.*[12] have made a research on epitaxial PZT (20/80) thin films with different top electrodes. They revealed that diode-like current behavior found in their devices was not switchable with the reversal of polarization. However, in this paper we explored electrical conduction in polycrystalline $Pb(Zr_{0.53}Ti_{0.47})O_3$ (PZT) thin film with the structure of Pt-PZT-Au. Switchable ferroelectric diode effect in PZT thin film has been observed in our device, which exhibits great rectifying behavior. The conducting direction can be reversed by switching the direction of the polarization in the PZT film. Besides, polarization-tuned and temperature-tuned conductive characteristics have also been completely studied in our sample.

II. EXPERIMENT

The thin film of PZT was deposited on Pt(200nm)/Ti(50nm)/SiO_2(500nm)/Si substrates *via* chemical solution deposition method. Before preparation of PZT film, the substrate was cleaned following the standard wafer cleaning procedure. Lead acetate trihydrate ($Pb(CH_3CO_2)_2{\cdot}3H_2O$), Titanium *n*-butoxide ($Ti(O\text{-}nBu)_4$) and Zirconium *n*-butoxide ($Zr(O\text{-}nBu)_4$) were employed as raw materials, and 2-methoxyethanol and acetylacetone (ACAC) were used as solvent and stabilizer, respectively. All chemical reagents with analytical purity were purchased from Sinopharm Chemical Reagent Co., Ltd. First of all, Lead acetatetrihydrate was dissolved in 2-methoxyethanol, then refluxed at 105 °C for 30 min under stirring to remove the hydration water. After cooling, Titanium *n*-butoxide and Zirconium *n*-butoxide were dipped in until desired stoichiometric ratio. Then a certain amount of acetylacetone was added into the mixed solution, so as to make the precursor stable. 10% mole excess lead acetate was added in order to compensate the loss in the procedure of heat treatment and the concentration of the final precursor solution was adjusted to 0.5 M. The detailed process of preparing the precursor solution also can be found somewhere else.[13–15] The coating solution was dipped on Pt/Ti/SiO_2/Si substrate and spin-coated at 4000 rpm for 30 s, then the precursor film was dried at 400 °C for 5 min for pyrolysis. These processes were repeated for several times until the desired thickness is obtained. At last, the PZT film was annealed at 700 °C for 1 hour in an electric furnace. Both the procedures of pre-fire and anneal were carried out in the stable air atmosphere.

The structure and crystalline phase of the PZT film by X-ray diffraction (XRD) (RIGAKU, model: D-MAX 2200 VPC) was carried out using filtered Cu $K_{\alpha 1}$ radiation (λ = 0.154 nm) operated at voltage 30 kV and current 30 mA. The thickness of the sample was tested by JEOL scanning electron microscope (SEM) (model: JSM-6330F). Surface morphology and domain structures were investigated by scanning probe microscope (SPM) (Being Nano-Instruments Ltd., model: CSPM5500). To measure electrical properties, Au top electrodes with diameter of 0.5 mm were deposited by ion sputtering with a mask. Radiant Precision Multiferroic Materials Analyzer (Multiferroic 100V) was used to measure the ferroelectric polarization and carry out the pre-poling process. Current density vs. voltage (*J*-*V*) curves and capacitance vs. voltage (*C*-*V*) curves was detected by Keithley 4200 semiconductor characterization system (SCS). An Agilent source meter (Model: 33220A) and an oscilloscope from Tektronix Inc. was used in switching current tests. In temperature dependence measurements of ferroelectric hysteresis loops and *J*-*V* curves, the temperature was controlled by Linkam T96-PE temperature platform. The polarity of the applied voltage was defined with reference to the bottom electrode in all cases.

All article content, except where otherwise noted, is licensed under a Creative Commons Attribution 3.0 Unported license. See: http://creativecommons.org/licenses/by/3.0/ Downloaded to IP: 113.96.155.10 On: Tue, 09 Dec 2014 06:41:23

III. RESULTS AND DISCUSSIONS

Fig. 1(a) shows the XRD pattern measured with the scan speed of 6° min^{-1} in range of 20° ~ 60°. The XRD pattern confirms that the sample has pure phase of $Pb(Zr_{0.53}Ti_{0.47})O_3$ with space group of *P*4*mm* (JCPDS card No. 70-4264), indicating that the PZT film is polycrystalline film in tetragonal phase without preferred growth direction. The thickness of the PZT film is estimated to be about 600 nm from cross section image detected by scanning electron microscopy (SEM), as showed in Fig. 1(b). Fig. 1(c) presents the surface morphology tested by using AFM in an area of 4×4 μm^2, and shows that the top surface is smooth with an average roughness of the order of 3 nm. Fig. 1(d) shows the schematic of the final measuring system after Au top electrodes is deposited on the surface of PZT thin film.

In order to attain accurate ferroelectric characteristics of PZT film excluding the polarization caused by leakage current, "Remanent Hysteresis" mode of Radiant Precision Analyzer is used to investigate the hysteresis loops at room temperature. Fig. 2(a) shows the polarization-voltage (*P*-*V*) curves of the PZT thin film with increasing applied voltage. It is noted that all *P*-*V* curves are measured with a triangular wave format with frequency 2 kHz in our work. The rectangular hysteresis loops indicate that the PZT film exhibit good ferroelectric characteristics. Due to the asymmetrical electrode structure used in this work, a built-in electric field forms in the MFM device and results in asymmetrical shape of hysteresis loop, which is familiar in asymmetrical MFM devices[16,17] The coercive voltage ($+V_c$) at positive bias is about 3.2 V, while at negative bias it is about -3.0 V. The coercive voltages scarcely change with the increase of applied voltage. Nevertheless, the remanent polarizations (P_r) increase with the applied voltage and are close to saturation when the voltage reaches 15V. The remanent polarization could reach 30 $\mu C\ cm^{-2}$. Compared with other work on PZT film, our results unveil that smaller coercive voltages and higher remanent polarization exist in our PZT sample.[17–19] Fig. 2(b) shows the piezoresponse phase image of piezoresponse force microscope (PFM) on a 4×4 μm^2 area. For this measurement, a voltage of 2 V with 17 kHz was applied to Au-coated tip (Budget Sensors ContGB, tip radius: < 25 nm). We define the orientation of polarization towards Au top electrode as P_{up}, on the other hand, the orientation of polarization towards Pt bottom electrode is defined as P_{down}. The bright region (P_{up}) is attained by applying -10 V scanning bias, and a sequential poling with +10 V bias on the dark region (P_{down}) reverses the polarization from P_{up} to P_{down}. The piezoresponse signal indicates that domain structure is stable and can be switched by the external electric field, which is important to analyze the effect of

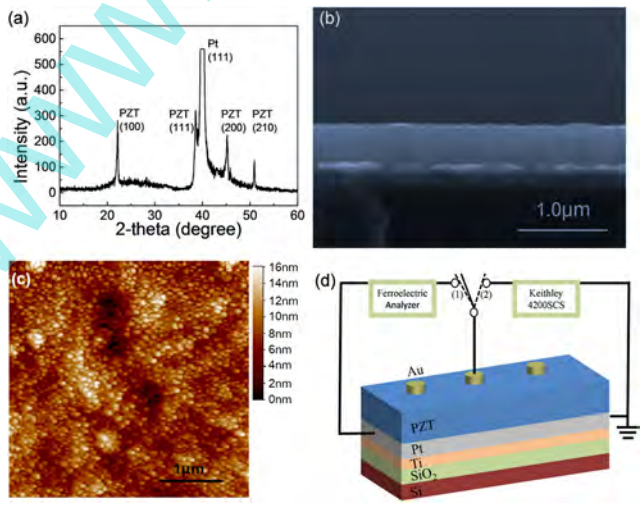

FIG. 1. (a) XRD pattern of $Pb(Zr_{0.53}Ti_{0.47})O_3$ on Pt(111)/Ti/SiO_2/Si substrate, (b) and (c) are cross section image and surface topography tested by SEM and atomic force microscope, respectively. (d) Schematic device structure of Au/PZT/Pt capacitor and bottom electrode Pt is reference electrode in all conduction measurements. In (d) we have labeled the measurement sequence. (1) At first, the sample is pre-polarized by ferroelectric analyzer, (2) then *J*-*V* curves are collected by Keithley 4200SCS.

All article content, except where otherwise noted, is licensed under a Creative Commons Attribution 3.0 Unported license. See: http://creativecommons.org/licenses/by/3.0/ Downloaded to IP: 113.96.155.10 On: Tue, 09 Dec 2014 06:41:23

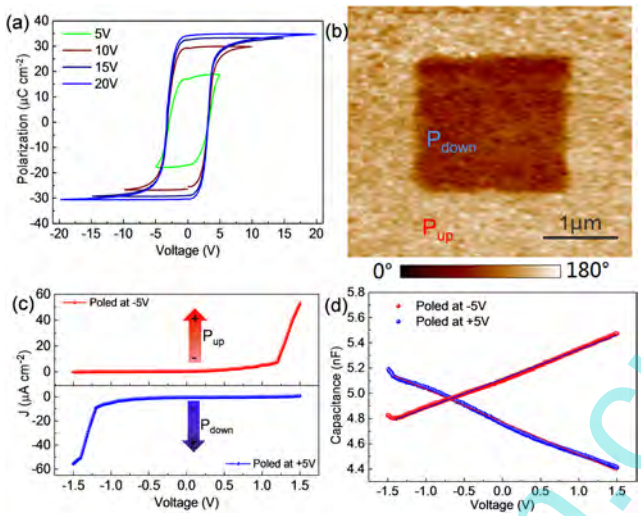

FIG. 2. (a) hysteresis loops at different applied voltages with 2 kHz frequency, (b) phase image of PZT film from PFM, (c) Switchable ferroelectric diode phenomenon in PZT film. Current density - voltage (J-V) characteristic in the range of -1.5 V to +1.5 V shows rectifying behavior and the polarity of the forward/reverse bias can be reversed by changing the orientation of the polarization; (d) C-V curves after the film is poled at +5V and -5V, respectively. C-V curves are measured at 2 kHz.

polarization on the SFDE of the PZT thin film, and discussed in the following section III A. Fig. 2(c) presents the J-V curves measured by applied voltage on Au top electrodes. In order to measure effect of a stable polarization on the SFDE and avoid the polarization switching, all measurements are carried out in voltage range between -1.5 V to 1.5 V below the coercive voltage of the PZT thin film. In J-V measurements, the applied voltage is stepwise swept from -1.5 V to 1.5 V with interval of 0.01 V, while a delay time of 2 s is used to set the voltage steps and read the current. The results reveal that after poling the sample with -10 V bias (P_{up} state), the J-V curve shows rectifying behavior and exhibits positive-forward diode, whereas after poled at +10 V the J-V curve shows negative-forward diode.

So as to verify whether the current presented in Fig. 2(c) is leakage current or just the polarization switching current, we carry on two further measurements on switching current and C-V curves within the range of -1.5 V and 1.5 V. The schematic measurement circuit is shown in Fig. S1(a) (see Support information).[20] The series resistance (R) is 10 Ω, which is much smaller than the resistance of ferroelectric film. The width of applied pulse for pre-polarization and measurement of switching current is 50μs, which is much larger than the time of domain switch. Fig. S1(b)[20] shows the transient current measured at 5 V and 10 V, respectively. It could prove that circuit is competent to the test of switching current. Then the transient current at -1.5 V is collected after the desired poling voltage. In order to confirm whether the domain switch occurs at -1.5 V or not, charging current and discharging current is compared with each other. As shown in Fig. S1(e) and S1(f),[20] we find that the difference between the charging and discharging current is negligible alike the condition occurred in capacitance. These results indicate the domain switching is hardly involved in electrical transport. On the other hand, since diode-like electrical behaviors are obtained in Fig. 2(c), C-V characteristic from -1.5 V to +1.5 V should present as linear as reported by L. Pintilie *et al.*[21] Fig S2(a) and (b)[20] present the C-V curves tested from +1.5 V to -1.5 V then back to +1.5 V poled at +5V and -5V, respectively. It is worth to note that the applied voltage is swept up from -1.5 V to +1.5V in J-V measurements. From the C-V curves shown in Fig 2(d), it is obvious that the obtained characteristics are linear when the voltage sweeps up from -1.5 V to +1.5 V. In brief, we could infer that domains are hardly switched in 1.5 V and one Schottky barrier exits in Pt-PZT-Au structure after pre-polarization. As reported on BFO films, the SFDE is attributed to the polarization-induced asymmetric band-bending at the two electrode interfaces and results in one Schottky barrier in one of the two interfaces.[3,8–11,22] At virgin state without poling, metal-ferroelectric-metal (MFM) structure based on n type films can be modeled as a back-to-back

All article content, except where otherwise noted, is licensed under a Creative Commons Attribution 3.0 Unported license. See: http://creativecommons.org/licenses/by/3.0/ Downloaded to IP: 113.96.155.10 On: Tue, 09 Dec 2014 06:41:23

connection of two Schottky diodes at the interfaces between two electrodes and ferroelectric. When the ferroelectric thin film is poled to up state, metal contact and Schottky contact are caused by the positive and negative polarization charges, respectively. Vice versa when polarization is reversed and the polarity of the diode switches.

However, PZT films fabricated by spin coating method are generally considered as p-type semiconductor according to the lead vacancies.[23–25] In our case, the work function of Pt is taken as 5.3 eV and that of Au is 5.1 eV.[23,26] As for PZT film, the band gap E_g is 3.4 eV, and the electron affinity is taken as 2.15 eV.[27,28] Therefore, when PZT and Pt or Au are joined, the barrier height at the Pt/PZT interface is about 0.25 eV for holes, and that at the Au/PZT interface is about 0.45 eV. Some electrons in the two electrodes should move spontaneously into PZT film due to the higher Fermi level of Pt or Au than that of PZT, and leave behind positive charges in Pt and Au electrodes. Then depletion regions are formed in PZT near the bottom and top electrodes, respectively. Built-in field is set up from electrodes towards the PZT thin film, and results in face-to-face connection of Schottky diodes at zero bias that is different from n-type BFO film (back-to-back connection) as mentioned above, as shown in Fig. 3(a). When the ferroelectric film is poled to P_{up} state, the positive polarization charges can neutralize the electrons diffused from Au top electrode and then induce upward band bending (the decrease of barrier height and depletion region for holes), resulting in metal contact. At the interface between PZT and Pt, the negative charges at the tail side of the polarization would simultaneously increase the charge density, leading to downward band bending and the increase of barrier height and depletion region. Therefore, in P_{up} case, an enhanced Schottky barrier at the interface between PZT and Pt leads to the aforementioned unidirectional rectifying behavior. Fig 3(b) schematically shows the modulated band structure for the P_{up} case at zero bias. As the P_{down} case, reverse phenomena occur at the two interfaces, i.e., band bends down at the Au/PZT interface, and band bends up at the PZT/Pt interface, as shown in Fig. 3(c). In brief, when the BFO film is pre-polarized, the direction of forward voltage is the same as the direction of remnant polarization while the direction of forward voltage after PZT is pre-polarized is opposite to the direction of remnant polarization.

Furthermore, according to the model of metal-ferroelectric interface proposed by L. Pintilie *et al.*[21,25] and M. S. Jang *et al.*,[13] the variation in the built-in potential modulated by ferroelectric polarization can be given by $\Delta\delta_{bi}^{P} = \delta'_{bi} - \delta_{bi} = \pm P\delta/\varepsilon_0\varepsilon$, where δ'_{bi} is the apparent built-in potential with contribution from polarization, δ_{bi} is the built-in potential without contribution from polarization, P is the ferroelectric remanent polarization, δ is the distance between the polarization sheet of charge and the physical metal-ferroelectric interface, ε_0 and ε is the permittivity of vacuum and the static dielectric constant of the ferroelectric, respectively. For our case, ε measured by frequency dependent capacitance curve is ~840 and δ is taken as 12 nm.[29] From the hysteresis loops in Fig. 2(a), the remanent polarizations after poled by +5 V and -5 V are about 17 μC·cm^{-2}. The corresponding variations in the built-in potential $\Delta\delta_{bi}^{P_{down}}$ and $\Delta\delta_{bi}^{P_{up}}$ caused by polarization are about ±0.257 eV. Because the moderate barrier heights in the two interfaces at zero bias are $\delta_{B\text{-}Pt}$=0.25 eV and $\delta_{B\text{-}Au}$=0.45 eV, the polarization bends the energy bands to metal contact at Pt interface and keep the energy bands at Au interface in Schottky contact when the PZT film is poled down by +5 V.

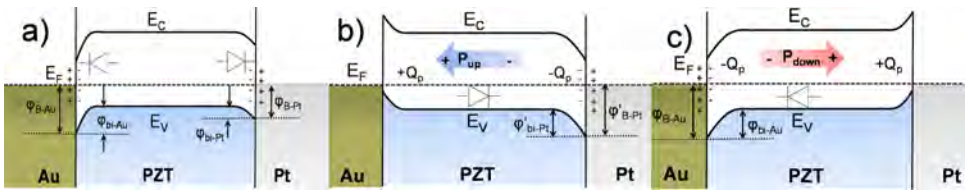

FIG. 3. Schematic energy band diagrams illustrating the variations in Schottky barriers from face-to-face diodes at virgin state (a) to a positive-forward diode at P_{up} state (b) and to a negative-forward diode at P_{down} (c), corresponding to the J-V curves in Fig. 2(c), respectively. Where, $\varphi_{B\text{-}Pt}$ ($\varphi_{B\text{-}Au}$) is the Schottky barrier at bottom (top) interface; $\varphi'_{B\text{-}Pt}$ ($\varphi'_{B\text{-}Au}$) is Schottky barrier at bottom (top) with polarization; Q_p is polarization charge; $\varphi_{bi\text{-}Pt}$ ($\varphi_{bi\text{-}Au}$) is built-in potential barrier near the electrodes.

All article content, except where otherwise noted, is licensed under a Creative Commons Attribution 3.0 Unported license. See: http://creativecommons.org/licenses/by/3.0/ Downloaded to IP: 113.96.155.10 On: Tue, 09 Dec 2014 06:41:23

With the increase of poling voltage, more residual polarization exits in PZT film as shown in Fig. 2(a), and are sufficient to bend the bands at Au interface, resulting in metal contact.

A. Effect of the remanent polarization on the SFDE in PZT thin film

In order to obtain additional information of SFDE as a function of remanent polarization (P_r), we apply 5 rectangular voltage pulses to reach a stable polarization. Each pulse has width of 5 ms, which is large enough for domain relaxation. At first, we use positive pulses +5 V to pole the sample toward bottom Pt electrode (P_{down} state), then the corresponding *J-V* measurement is carried out in low bias voltage from -1.5 V to +1.5 V. Sequentially, negative pulses -5 V is applied in order to switch the polarization toward top Au electrode (P_{up} state), and *J-V* curve is measured in the same bias region. In addition, poling pluses with larger voltages, e.g., +10 V, -10 V, +15 V and -15 V, are also applied on the sample. After each poling process, *J-V* curve is collected from -1.5 V to +1.5 V. All measurements in this section are performed at room temperature. The polarization as function of pulse voltage and measurement sequence is shown in Fig. 4(a) and 4(c) for P_{down} state and P_{up} state, respectively. The corresponding *J-V* curves after different pulse voltage poling for the two polarization states are shown in Fig. 4(b) and 4(d). Interestingly, it is found that the forward current of the SFDE gradually decrease with the increase of the polarization in PZT thin film.

In general, ferroelectric domain walls (DWs) and grain boundaries play the main part of conductive channels in ferroelectric devices.[30–33] Nevertheless, the grain boundaries are unlikely to be affected in our tests and could be excluded from the origin of forward current reduction at larger polarization. With the increase of poling voltage, small domains would merge into big domains to increase the remanent polarization.[30] In other words, the amount of domain walls that take important part in conduction might decrease with the increase of poling voltage. Hence, forward currents of both positive diode and negative diode are likely to decrease when the remanent polarization increases. On the other hand, according to the model discussed in the above section,

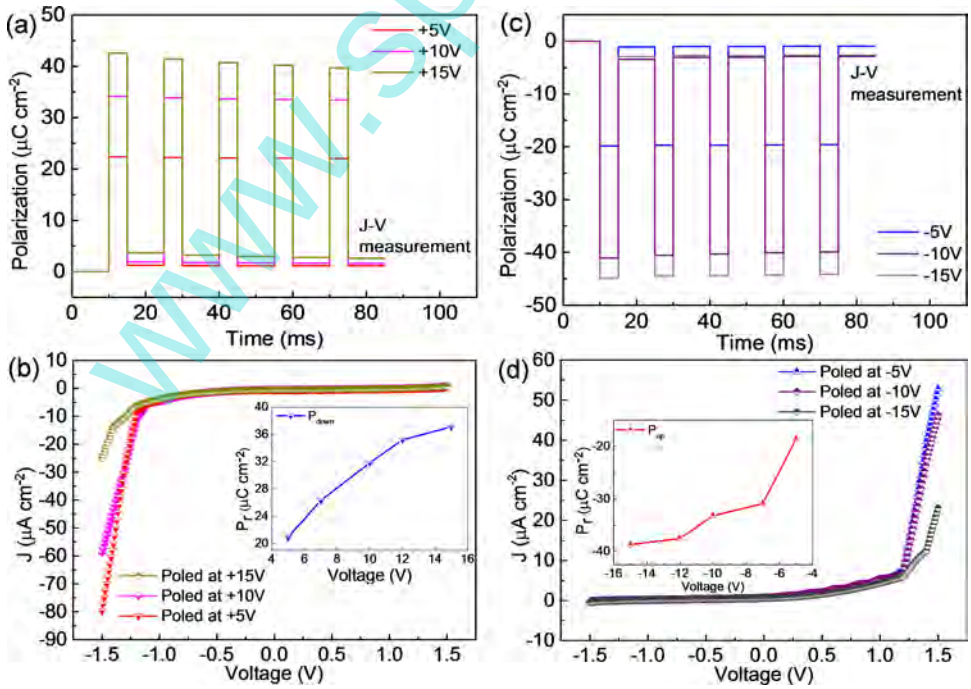

FIG. 4. Polarization as function of pulse voltage and measurement sequence for (a) P_{down} state and (b) P_{up} state. *J-V* curves measured after applying 5 voltage pulses for (c) P_{down} state and (d) P_{up} state. Insets in (b) and (d) indicate the corresponding polarization as function of voltage.

All article content, except where otherwise noted, is licensed under a Creative Commons Attribution 3.0 Unported license. See: http://creativecommons.org/licenses/by/3.0/ Downloaded to IP: 113.96.155.10 On: Tue, 09 Dec 2014 06:41:23

the variation of barrier height is directly proportional to the ferroelectric polarization. The increase of built-in potential in Pt-PZT-Au structure due to increment of the remanent polarization results in more hindrance for the injection of holes from electrodes. Therefore, the polarization dependence of Pt-PZT-Au conduction might be a combined effect of domain walls conductivity and barrier height modulated by polarization.

B. Effect of temperature on the SFDE in PZT thin film

In order to investigate the influence of the temperature on SFDE, we measure the ferroelectric characteristics and the *J-V* curves after electrical poling. The ferroelectric hysteresis loops dependent on temperature are performed at voltage 10 V and frequency 2 kHz as shown in Fig. 5(a). It can be seen from Fig. 5(b) that the remanent polarization (P_r) and coercive voltage (V_c) reduce as temperature gradually increases from 150 K to 450 K. *J-V* measurements after positive electrical poling at +10V and negative poling at -10 V are displayed in Fig. 5(c) and 5(d), respectively. With temperature increasing, the maximum forward current (I_{+max}) increase correspondingly. In negative

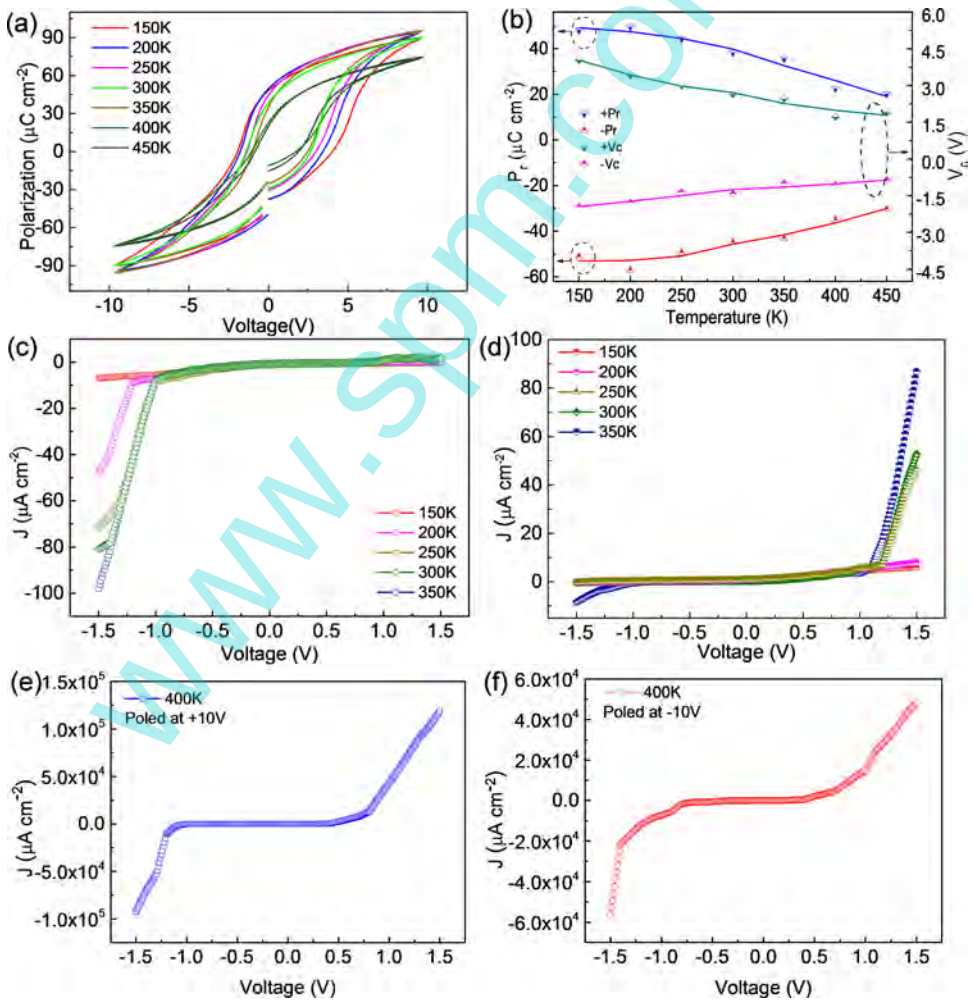

FIG. 5. (a) hysteresis loops in temperature range of 150 K to 450 K measured at 10 V periodic voltage with frequency 2 kHz, (b) remanent polarization and coercive voltage as function of temperature, (c), (d) *J-V* curves measured after poling at +10 V and -10 V, in temperature range of 150 K to 350 K, (e) and (f) *J-V* curves measured at 400 K, after poling at +10 V and -10 V, respectively.

www.spm.com.cn

All article content, except where otherwise noted, is licensed under a Creative Commons Attribution 3.0 Unported license. See: http://creativecommons.org/licenses/by/3.0/ Downloaded to IP: 113.96.155.10 On: Tue, 09 Dec 2014 06:41:23

diode (poled at +10 V), I_{+max} at -1.5 V increase from about 7 μA·cm^{-2} at 150 K to 99 μA·cm^{-2} at 350 K, while I_{+max} at +1.5 V increase from about 6 μA·cm^{-2} at 150 K to 86 μA·cm^{-2} at 350 K in positive diode (poled at -10 V). The maximum reverse currents (I_{-max}) also increase as temperature increased, but the magnitude is not obvious. Besides, the maximum rectification ratio ($|I_{+max}|/|I_{-max}|$) is about 220 observed at 250 K,and it is much bigger than the rectification ratio of BFO films reported previously.[3,6]

When the temperature reaches 400 K, the *J*-*V* curves are almost symmetric no matter the sample is poled at positive voltage or negative voltage, as shown in Fig. 5(e) and 5(f), respectively. This symmetric conduction characteristic is mainly caused by the thermally activated charge carriers[34] rather than the vanishing of polarization, since there is still significant polarization in the sample at 400 K, as shown in Fig. 5(a). As a p type semiconductor, the carrier concentration and mobility decrease with the decrease of temperature, which lead to the minor diode behavior in 150K. When the temperature increases, electrons from oxygen vacancies or even some electrons in valence band can be excited into conduction band, and the depletion region becomes thinner, both of which contribute to a larger current density under the same voltage bias.[31,35] Also reported in literature,[23] when the temperature increases from 300 K to 375 K, free carrier density increases up to three order of magnitude both in forward bias and negative bias and the dominating electrical mechanism in PZT film changes from space-charge-limited bulk conduction (SCLC) to interface-limited Schottky emission (SE) at 375 K.

C. Conduction mechanisms

After understanding the detailed physical mechanism of SFDE formation in the PZT film, we further analyze conduction mechanism of SFDE though mathematical fitting the *J*-*V* curves according to some reported conduction mechanisms. For our sample, three conduction mechanisms are possible. They include space-charge-limited bulk conduction (SCLC), interface-limited Schottky emission (SE) and bulk-limited Poole-Frenkel hopping (PF).

Regarding to SCLC conduction model, it is bulk limited effect assuming carriers travelling through the film thickness rather than limited carrier injection from the electrode.[36–38] In general, the form of SCLC current is proportional to a power function of the applied voltage ($J \propto V^n$). At low voltage, electrical conduction shows Ohmic behavior (region I, $n \approx 1$), as carries are injected from electrodes to fill the traps. As the voltage increases, swallow traps are fully filled and create an internal electrical field against the applied field, which limits the injection of carries (region II, $n \approx 2$). Then deep traps are also filled with a further increase of applied voltage, and in this region exponent n is larger than 2 (region III). Once the deep traps are fully filled, the injection of carries is again limited by the internal electrical field created by carriers filled in traps (region IV, $n \approx 2$).[39] Specifically, the current density can be described in following equation,[32,36]

$$J = \frac{9\theta_f \varepsilon_0 \varepsilon_r \mu V^2}{8d^3} \tag{1}$$

where θ_f is the fraction of injected carriers (i.e., not trapped), ε_0 is the permittivity of vacuum, ε_r is the relative dielectric constant of the film, μ is the carries mobility, V is the applied voltage and d is the film thickness. To analyze this conduction mechanism, we can fit the *J*-*V* curves in the form of log(*J*) *vs*. log(*V*) to find reasonable n. Fig. 6(a) shows the log(*J*) *vs*. log(*V*) plots for P_{up} state poled at -5 V. In negative bias, n is fitted to be 1, indicating the Ohmic conduction. Moreover, there are three linear fitting in positive bias. In region of $0<\log(V)<-1$, n is about 0.9, indicating that the conduction is still in Ohmic feature. In moderate bias region, n is fitted to be 1.9, which is compatible with the non-trapped case and satisfies the power-law dependence. When $\log(V)>0$, the fitted n is about 8.7, which seems satisfy the above-mentioned region III of SCLC. However, it is also possible that it changes to another conduction mechanism (see in the following). Since 1.5V is close to the coercive field, the sample cannot suffer larger applied voltage without polarization reversal, and the existence of region IV of SCLC cannot be inferred from the log(*J*) *vs*. log(*V*) plots.

All article content, except where otherwise noted, is licensed under a Creative Commons Attribution 3.0 Unported license. See: http://creativecommons.org/licenses/by/3.0/ Downloaded to IP: 113.96.155.10 On: Tue, 09 Dec 2014 06:41:23

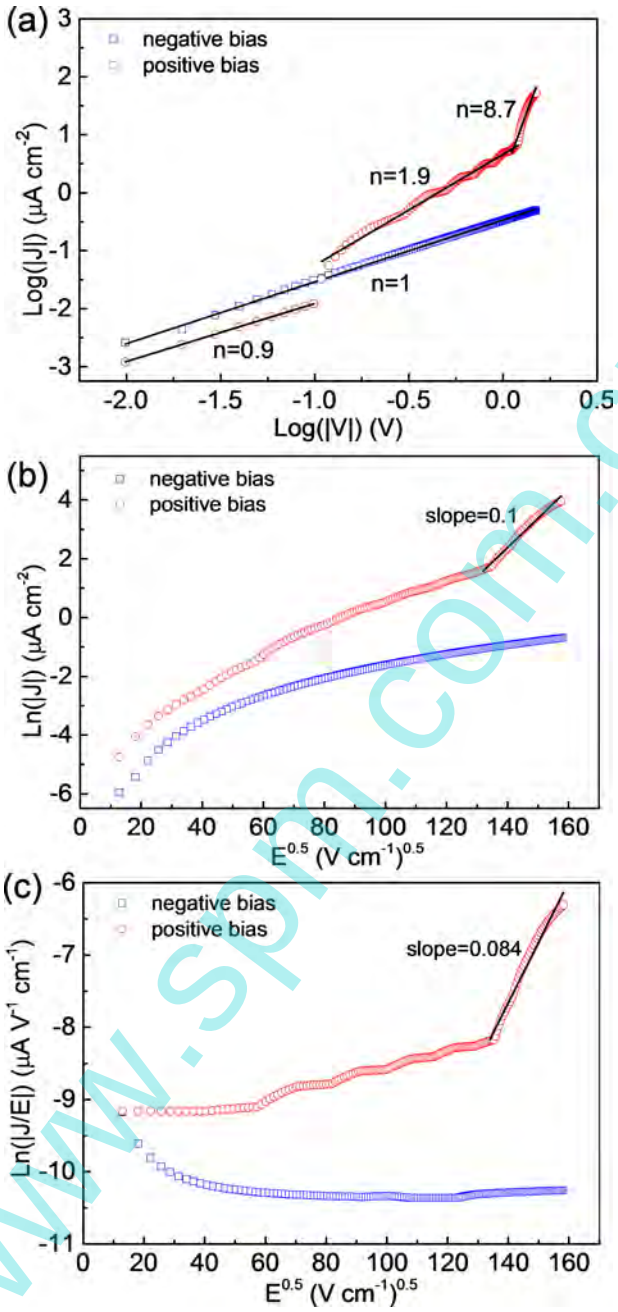

FIG. 6. (a) log(|J|) *vs.* log(|V|) plots for space charge limited conduction (SCLC) mechanism, solid lines are the fitting curves (b) ln(J) vs. $E^{0.5}$ plots for Schottky emission (SE) mechanism; (c) ln(J/E) *vs.* $E^{0.5}$ plots for Poole-Frenkel (PF) hopping. All of them are mathematical treatment of the J-V curve with the upward polarization state poled at -5 V.

As for Schottky emission (SE), the relationship between current density and field intensity can be described as,[18,37]

$$J_{SE} = A^* T^2 \exp\left(-\frac{\varphi - \sqrt{q^3 E/4\pi\varepsilon_0\varepsilon_r}}{k_B T}\right) \quad (2)$$

where A^* is the Richardson constant, T is the temperature, φ is the height of the Schottky barrier, q is the electronic charge, and k_B is the Boltzmann constant. It is worth to note that there is a controversy whether ε_r is relative dielectric constant or optical dielectric constant.[40] For ferroelectrics,

All article content, except where otherwise noted, is licensed under a Creative Commons Attribution 3.0 Unported license. See: http://creativecommons.org/licenses/by/3.0/ Downloaded to IP: 113.96.155.10 On: Tue, 09 Dec 2014 06:41:23

polarization may play important part in shielding the electrical field and contribute to the apparent value of ε_r. As presented in the above equation, the data should display the linear behavior of a $\ln(J)$ *vs.* $E^{0.5}$ plots. Thus, we analyze the J-V curve for the P_{up} state after poled at -5 V, as shown in Fig. 6(b). No reasonable line is observed in most region of the curve. However, an attempt to obtain the value of ε_r by linearly fitting a limited region of $135<E^{0.5}<160$ gives that $\varepsilon_r \approx 216$, which is much greater than reported optical dielectric constant of PZT films.[18,40] Nevertheless, it is smaller than and in the same order of our measured static dielectric constant of PZT ($\varepsilon = 840$). Considering the decrease of dielectric constant of ferroelectrics as applied bias increases, $\varepsilon_r \approx 216$ seems reasonable in the region of $135<E^{0.5}<160$. Hence, Schottky barrier limited conduction seems also possible in the aforementioned electrical region.

Moving to Poole-Frenkel hopping, the current density as a function of field intensity could be expressed as,[41]

$$J_{PF} = BE\exp\left(\frac{-E_l - \sqrt{q^3E/\pi\varepsilon_0\varepsilon_r}}{k_BT}\right) \tag{3}$$

Where B is the constant, E_l is the trap ionization energy. The relationship between $\ln(J/E)$ and $E^{0.5}$ should be fitted in a line. Then we analyze the same J-V curve as aforementioned. The result is shown in Fig. 6(c). We cannot obtain a reasonable linear fitting in most region of curve for the PF emission model. An attempt to fit the limited region of $135<E^{0.5}<160$ results in $\varepsilon=1.2\times10^9$, which is illogical for PZT thin film. Hence, we can exclude the PF hopping for the conduction mechanism in our sample.

IV. CONCLUSIONS

In summary, we have demonstrated a pronounced switchable ferroelectric diode effect (SFDE) in polycrystalline PZT thin film fabricated by chemical solution deposition method. Polarization-modulated barrier height in the interface between ferroelectric and metal electrodes induces the switching of the ferroelectric diode. Result shows that J-V curves could be controlled by the remanent polarization and temperature. In particular, with the increase of remanent polarization, the decrease of domain walls and the increase of built-in potential contribute to the reduction of forward current. Furthermore, high temperature will diminish the current rectification. The space-charge-limited conduction (SCLC) mechanism is most likely to control the carrier injection from the electrodes. Our results proved that SFDE is universal property of the ferroelectric structures with appropriate Schottky contacts and is instructive for exploring pronounced switchable diode effect for non-destructive read-out FeRAMs.

ACKNOWLEDGEMENTS

The authors acknowledge the financial support of NSFC (51172291, 11072070, 11474363) and Shenzhen Research Foundation (JC201104210044A, ZYC201105160169A, ZDSY20120613125247154, JCYJ20120613133835232), Yue Zheng also thanks the Fundamental Research Funds for the Central Universities, New Century Excellent Talents in University, Research Fund for the Doctoral Program of Higher Education, and Fok Ying Tung Foundation, Science and Technology Innovation Project of Guangdong Provincial Education Department and Guangdong Natural Science Funds for Distinguished Young Scholar.

[1] J. F. Scott, Science **307**, 954–959 (2007).
[2] Y. A. Park, K. D. Sung, C. J. Won, J. H. Jung, and N. Hur, J. Appl. Phys. **114**(9), 094101 (2013).
[3] C. Wang, K.-j. Jin, Z.-t. Xu, L. Wang, C. Ge, H.-b. Lu, H.-z. Guo, M. He, and G.-z. Yang, Appl. Phys. Lett. **98**(19), 192901 (2011).
[4] P. Maksymovych, S. Jesse, P. Yu, R. Ramesh, A. P. Baddorf, and S. V. Kalinin, Science **324**(5933), 1421–1425 (2009).
[5] R. Guo, L. You, Y. Zhou, Z. Shiuh Lim, X. Zou, L. Chen, R. Ramesh, and J. Wang, Nat. Commun. **4**, 1990 (2013).
[6] T. Choi, S. Lee, Y. J. Choi, V. Kiryukhin, and S. W. Cheong, Science **324**(5923), 63–66 (2009).
[7] C. H. Yang, J. Seidel, S. Y. Kim, P. B. Rossen, P. Yu, M. Gajek, Y. H. Chu, L. W. Martin, M. B. Holcomb, Q. He, P. Maksymovych, N. Balke, S. V. Kalinin, A. P. Baddorf, S. R. Basu, M. L. Scullin, and R. Ramesh, Nat. Mater. **8**, 485–493 (2009).

All article content, except where otherwise noted, is licensed under a Creative Commons Attribution 3.0 Unported license. See: http://creativecommons.org/licenses/by/3.0/ Downloaded to IP: 113.96.155.10 On: Tue, 09 Dec 2014 06:41:23

[8] A. Q. Jiang, C. Wang, K. J. Jin, X. B. Liu, J. F. Scott, C. S. Hwang, T. A. Tang, H. B. Lu, and G. Z. Yang, Adv. Mater. **23**(10), 1277–1281 (2011).
[9] D. Lee, S. H. Baek, T. H. Kim, J. G. Yoon, C. M. Folkman, C. B. Eom, and T. W. Noh, Phys. Rev. B **84**(12), 125305 (2011).
[10] S. Hong, T. Choi, J. H. Jeon, Y. Kim, H. Lee, H. Y. Joo, I. Hwang, J. S. Kim, S. O. Kang, S. V. Kalinin, and B. H. Park, Adv. Mater. **25**(16), 2339–2343 (2013).
[11] C. Ge, K.-J. Jin, C. Wang, H.-B. Lu, C. Wang, and G.-Z. Yang, Appl. Phys. Lett. **99**(6), 063509 (2011).
[12] L. M. Hrib, A. G. Boni, C. Chirila, I. Pasuk, I. Pintilie, and L. Pintilie, J. Appl. Phys. **113**(21), 214108 (2013).
[13] Y. S. Yang, S. J. Lee, S. H. Kim, B. G. Chae, and M. S. Jang, J. Appl. Phys. **84**(9), 5005 (1998).
[14] I. Chilibon and J. N. Marat-Mendes, J. Sol-Gel Sci. Techn. **64**(3), 571–611 (2012).
[15] D. S. L. Pontes, L. Gracia, F. M. Pontes, A. Beltrán, J. Andrés, and E. Longo, J. Mater. Chem. **22**(14), 6587 (2012).
[16] N. Sama, R. Herdier, D. Jenkins, C. Soyer, D. Remiens, M. Detalle, and R. Bouregba, J. Cryst. Growth **310**(14), 3299–3302 (2008).
[17] H. Miyazaki, Y. Miwa, and H. Suzuki, Mater. Sci. Eng., B **136**(2-3), 203–206 (2007).
[18] G. L. Rhun, G. Poullain, R. Bouregba, and G. Leclerc, J. Eur. Ceram. Soc. **25**(12), 2281–2284 (2005).
[19] L. Jiankang and Y. Xi, Mater. Lett. **58**(27-28), 3447–3450 (2004).
[20] See supplementary material at http://dx.doi.org/10.1063/1.4903772 for detail switching current measurement and futher data of C-V curves.
[21] L. Pintilie, V. Stancu, L. Trupina, and I. Pintilie, Phys. Rev. B **82**(8), 085319 (2010).
[22] Y. Yao, B. Zhang, L. Chen, Y. Yang, Z. Wang, H. N. Alshareef, and X. X. Zhang, J. Phys. D: Appl. Phys. **46**(5), 055304 (2013).
[23] T. P.-c. Juan, S.-m. Chen, and J. Y.-m. Lee, J. Appl. Phys. **95**(6)), 3120 (2004).
[24] M. V. Raymond and D. M. Smyth, J. Phys. Chem. Solids **57**(10), 1507–1511 (1996).
[25] L. Pintilie and M. Alexe, J. Appl. Phys. **98**(12), 124103 (2005).
[26] N. G. Apostol, L. E. Stoflea, G. A. Lungu, C. Chirila, L. Trupina, R. F. Negrea, C. Ghica, L. Pintilie, and C. M. Teodorescu, Appl. Surf. Sci. **273**, 415–425 (2013).
[27] P. Juan, Y. Hu, F. Chiu, and J. Y. Lee, J. Appl. Phys. **98**(4), 044103 (2005).
[28] H. Lee, Y. S. Kang, S.-J. Cho, B. Xiao, H. Morkoç, T. D. Kang, G. S. Lee, J. Li, S.-H. Wei, P. G. Snyder, and J. T. Evans, J. Appl. Phys. **98**(9), 094108 (2005).
[29] L. Pintilie, I. Boerasu, M. J. M. Gomes, T. Zhao, R. Ramesh, and M. Alexe, J. Appl. Phys. **98**(12), 124104 (2005).
[30] J. Seidel, P. Maksymovych, Y. Batra, A. Katan, S. Y. Yang, Q. He, A. P. Baddorf, S. V. Kalinin, C. H. Yang, J. C. Yang, Y. H. Chu, E. K. H. Salje, H. Wormeester, M. Salmeron, and R. Ramesh, Phys. Rev. Lett. **105**(19), 197603 (2010).
[31] E. A. Eliseev, A. N. Morozovska, G. S. Svechnikov, P. Maksymovych, and S. V. Kalinin, Phys. Rev. B **85**(4), 045312 (2012).
[32] R. K. Vasudevan, W. Wu, J. R. Guest, A. P. Baddorf, A. N. Morozovska, E. A. Eliseev, N. Balke, V. Nagarajan, P. Maksymovych, and S. V. Kalinin, Adv. Funct. Mater. **23**(20), 2592–2616 (2013).
[33] J. Guyonnet, I. Gaponenko, S. Gariglio, and P. Paruch, Adv. Mater. **23**(45), 5377–5382 (2011).
[34] S. R. Basu, L. W. Martin, Y. H. Chu, M. Gajek, R. Ramesh, R. C. Rai, X. Xu, and J. L. Musfeldt, Appl. Phys. Lett. **92**(9), 091905 (2008).
[35] H. T. Yi, T. Choi, S. G. Choi, Y. S. Oh, and S. W. Cheong, Adv. Mater. **23**(30), 3403–3407 (2011).
[36] G. W. Pabst, L. W. Martin, Y.-H. Chu, and R. Ramesh, Appl. Phys. Lett. **90**(7), 072902 (2007).
[37] X. Qi, J. Dho, R. Tomov, M. G. Blamire, and J. L. MacManus-Driscoll, Appl. Phys. Lett. **86**(6), 062903 (2005).
[38] H. Yang, M. Jain, N. A. Suvorova, H. Zhou, H. M. Luo, D. M. Feldmann, P. C. Dowden, R. F. DePaula, S. R. Foltyn, and Q. X. Jia, Appl. Phys. Lett. **91**(7), 072911 (2007).
[39] H. Hu and S. B. Krupanidhi, J. Mater. Res. **9**(6), 1484–1498 (1994).
[40] P. R. Emtage and W. Tantraporn, Phys. Rev. Lett. **8**(7), 267–268 (1962).
[41] Z. Chen, L. He, F. Zhang, J. Jiang, J. Meng, B. Zhao, and A. Jiang, J. Appl. Phys. **113**(18), 184106 (2013).

www.scirp.com.cn

All article content, except where otherwise noted, is licensed under a Creative Commons Attribution 3.0 Unported license. See: http://creativecommons.org/licenses/by/3.0/ Downloaded to IP: 113.96.155.10 On: Tue, 09 Dec 2014 06:41:23